Design and characterization of low-heat and low-alkalinity cements

M. Codina [a,d], C. Cau-dit-Coumes [b,*], P. Le Bescop [c], J. Verdier [d], J.P. Ollivier [d]

[a] ANDRA, Direction Scientifique, Service Colis/Matériaux, Parc de la Croix Blanche, 1-7 rue Jean Monnet, 92298 Châtenay-Malabry cedex, France
[b] Commissariat à l'Energie Atomique, DTCD/SPDE/L2ED, CEN Marcoule, 30207 Bagnols-sur-Cèze cedex, France
[c] Commissariat à l'Energie Atomique, DPC/SCCME/LECBA, CEN Saclay, 91191 Gif-sur-Yvette, France
[d] Laboratoire Matériaux et Durabilité des Constructions, INSA Toulouse, 135 avenue de Rangueil, 31077 Toulouse cedex 4, France

Abstract

Investigations were carried out to formulate and characterize low-alkalinity and low-heat cements which would be compatible with an underground waste repository environment. Several systems comprising Portland cement, a pozzolan (silica fume or fly ash) and blastfurnace slag were compared. All blends were characterized by high amounts of additions, the Portland cement (PC) fraction ranging only from 20 to 60%.

Cement hydration was studied using several techniques: X-ray Diffraction, TGA-DTA, calorimetry, pore solution extraction and microscopy. The most important result obtained with some ternary blends was the drop in the pore solution pH by more than one unit as compared with control samples elaborated with commercial cements. The alkali content (≈ 1 to 4 mmol/L) of the interstitial solution was also strongly reduced. The blends exhibited a low-heat output as required. Leaching tests carried out in pure water indicated a very slow decalcification of the samples. Several techniques such as optical microscopy, SEM/BSE, X-ray microanalysis or X-ray diffraction were compared to estimate the degraded thickness.

© 2007 Elsevier Ltd. All rights reserved.

Keywords: Waste management; Blended cements; Hydration; Pore solution; Durability

1. Introduction

The French Parliament Act of December 30 1991 defined three complementary lines of research with the objective to find a solution to manage high-level and intermediate-level long-lived radioactive wastes over the very long term. One of the options examined by Andra (The French National radioactive waste management agency) is to dispose radioactive wastes in deep geological structures. The disposal concepts are based on a multibarrier design approach. The barriers would be: the waste package (the waste and the material used to stabilise it in a suitable overpack), the engineered barrier inserted between the waste package and the rock, and the geological barrier, i.e. the actual rock [1].

Clay has been chosen to constitute the geological barrier for its low permeability, which leads to low water flow, and for its stability over geological time scales. Clay may also be used as a main component in the storage framework. For instance, swelling bentonite could be used to seal some tunnels in association with concrete. In this context, it has been pointed out that the clay properties may be altered by the high pH conditions of the cement pore water [1,2]. Moreover, a high temperature rise caused by cement hydration in massive concrete elements could induce microcracking with negative consequences on its long term durability. Investigations have thus been carried out to formulate low-alkalinity and low-heat blended cements referred as "low-pH" binders, which would show an improved compatibility with the repository environment and which could be used to elaborate high-strength concrete.

A list of specifications to be checked by the concrete materials has been defined including easy supply of the raw materials,

* Corresponding author.
E-mail address: celine.cau-dit-coumes@cea.fr (C. Cau-Dit-Coumes).

Table 1
Low pH blends developed in Canada, Sweden, Japan and Finland

	Canadian concrete [4]	Swedish concrete [5]	Japanese concrete [6]	Finnish grout [7,43]	
Blends composition	50% PC–50% SF	83.3% PC–16.7% SF	40% PC–20% SF–40% FA	56% PC–38% SF–1.5% gypsum–4.2% alumina cement	49% PC–46% SF–1.3% gypsum–3.7% alumina cement
Reference	LHHPC Low-Heat High Performance Concrete	36F	HFSC High Fly ash Silica fume Cement	f63	f64
pH of water equilibrated with crushed solid	10.6 90 days of curing, L/S=1 mL/g	11.7 28 days of curing, L/S=1.675 mL/g	11.0 28 days of curing, L/S=40 mL/g	10.5 58 days of curing, sample surface/ leachate volume=0.85 cm^2/mL, the solution was renewed with the following kinetic: 0.26 L/year, 140 days of leaching	
Use	Concrete used in the construction of seals for underground repositories (located in granite rock) for heat-generating, radioactive, nuclear wastes	Injection grouts to stabilise the rock in the fractured zones or stabilisation concrete that replaces excavated sections that have collapsed	Cementitious material used for plug, grout and rock bolts in deep repository	Injection grout for deep repositories	

pore solution pH around 11 and temperature rise during hydration less than 20 °C under semi-adiabatic conditions.

It has been shown that low-pH cements can be designed by replacing significant amounts of Portland cement (PC) by silica fume, which can be associated in some cases to low-CaO fly ash and/or blastfurnace slag [3–7] (Table 1). Such a blend has several positive effects: *(i)* conversion of portlandite, which is formed by the hydration of PC and which buffers the pore solution at pH 12.5, into calcium–silicate–hydrate (C–S–H) by the pozzolanic reaction [8], *(ii)* decrease in the CaO/SiO$_2$ ratio of the C–S–H and partial substitution of Al^{3+} for Si^{4+} in the silicate chains of the C–S–H, which enhances their sorption capacity of alkalis [9–14], and *(iii)* dilution of PC, which decreases the heat output during hydration. The pore solution pH of the cement paste is then controlled by the dissolution of the C–S–H gel: the lower the CaO/SiO$_2$ ratio of the C–S–H, the lower the pH [15] (Table 2).

Previous research was mainly focused on the use of low-pH binders to design materials for specific applications such as high-strength and/or low-heat concrete [3–5], or injection grout to seal cracks [7]. One concern in those studies was to check that conventional engineering practices could be used despite the unusually high content of silica fume and other additions in the binder. This work is devoted to the chemistry of low-pH binders during hydration and leaching. Cement pastes were prepared from five blends consisting in binary, ternary or quaternary mixes (Table 3) and characterized over a one-year period. 7 month-old samples were also submitted to leaching by pure water in order to compare their degradation rates and assess the mineralogical evolutions involved.

2. Experimental

2.1. Materials

Table 4 shows the composition of the products used to design the low-pH blends.

Two hydraulic compounds were tested (PC and blast furnace slag), as well as two pozzolans (Fly Ash (FA) and a more reactive one, Silica Fume (SF)). PC and slag were chosen for their low alkali content. SF was selected in a densified form for easier handling. The quaternary blend (PC/SF/FA/slag) was prepared by adding SF to a commercial ternary blend containing PC clinker, FA and slag (referred as CEM V according to European standard EN 197-1).

2.2. Methods

Cement pastes (W/C=0.5) were characterized using mercury intrusion porosimetry (Micromeritics Autopore III — investigated pressures ranging 0.8 to 53000 psia). Crystalline phases were identified using XRD (Siemens D8 — Copper anode

Table 2
Link between pH and C/S ratio (25 °C [15])

Solids	pH
Amorphous silica	6.38
Amorphous silica+C–S–H (0.8)	10.17
C–S–H (0.8)	10.88
C–S–H (0.8)+C–S–H (1.1)	10.91
C–S–H (1.1)	11.03
C–S–H (1.1)+C–S–H (1.8)	12.43
C–S–H (1.8)+CH	12.53
CH	12.52

Table 3
Composition of the investigated blends (weight %)

	PC	CEM V*	Silica fume	Fly ash	Slag
B	60%	–	40%	–	–
T1	37.5%	–	32.5%	30%	–
T2	37.5%	–	32.5%	–	30%
T3	20%	–	32.5%	–	47.5%
Q	–	60%	40%	–	–

CEM V*: comprising 22% slag, 22% fly ash and 55% clinker.

Table 4
Chemical composition (weight %) of the blends components

	PC[a]	CEM V[b]	SF[c]	FA[d]	Slag[e]	Calculated values for the blends				
						B	T1	T2	T3	Q
CaO	67.41	46.42	0.40	5.52	42.3	40.6	27.0	38.1	33.7	28.0
SiO$_2$	22.84	29.44	95.00	49.48	36.2	51.7	54.3	50.3	52.6	55.7
Al$_2$O$_3$	2.7	11.36	0.60	29.17	11.1	1.9	10.0	4.5	6.0	7.1
Fe$_2$O$_3$	1.84	3.20	<0.05	6.23	0.97	1.1	2.6	1.0	0.8	1.9
MgO	0.81	3.02	0.30	2.08	7.6	0.6	1.0	2.7	3.9	1.9
MnO	n.m.	0.11	n.m.	0.08	0.15					
Na$_2$O	0.14	0.21	<0.20	0.58	<0.20	0.2	0.3	0.2	0.2	0.2
K$_2$O	0.23	1.06	0.29	1.22	0.34	0.3	0.5	0.3	0.3	0.8
SO$_3$	2.23	2.81	<0.20	0.64	n.m.	1.4	1.1			1.8
S^{2-}	<0.01	0.16	<0.10	n.m.	0.9			0.3	0.5	0.1
P$_2$O$_5$	n.m.	0.58	n.m.	0.70	<0.70					
TiO$_2$	n.m.	0.64	n.m.	1.61	0.51					
Loss of ignition (1000 °C)	1.72	1.48	3.10	2.20	<0.10					

([a]Portland Cement CEM I (Lafarge, Le Teil), [b]CEM V/A (Calcia, Airvault), [c]densified silica fume ChrysoSilica, [d]fly ash, [e]blast furnace slag (Calcia, Ranville)). n.m. = not measured.

$\lambda_{K\alpha 1}$ = 1.54056 Å), and the portlandite content was estimated using TGA (TA-SDT 2960) from the loss of water between 460 °C and 510 °C. The hydrates from PC and low-pH cement pastes were characterized from their Si/Ca and Al/Ca ratios by performing X-ray microanalyses using energy dispersion spectroscopy (Philips XL PW6631/01 LaB$_6$ filament, accelerating voltage = 15 kV, and SEM-FEG).

The heat output during hydration was investigated on cement pastes (W/C = 0.4 except for Q, 0.45) using Langavant semi-adiabatic calorimetry (according to European standard EN 196-9). This method consisted in introducing a sample of freshly made grout into a cylindrical container having a volume of approximately 800 cm^3. The container was placed into a calibrated calorimeter (with a coefficient of total heat loss below 100 J h^{-1}.K^{-1} for a temperature rise of 20 K) in order to determine the quantity of heat emitted in accordance with the development of temperature. The temperature rise of the sample was compared with the temperature of an inert sample in a reference calorimeter. At a given point in time, the heat of hydration of the binder contained in the sample was calculated by summing the heat accumulated in the calorimeter and the heat lost into the ambient atmosphere throughout the period of the test.

The pore solutions of cement pastes cured for 2, 6 and 12 months in sealed bags at 20 °C (W/C = 0.5, cylindrical samples h = 10 cm and Ø = 6.7 cm) were extracted using pressure (WALTER BAI 102/3000 — HK4, applied strength within the range 0–1700 KN). Their pH value was measured with a high alkalinity pH electrode, and the Na$^+$, K$^+$, Ca^{2+} and SO$_4^{2-}$ concentrations were determined using ionic chromatography.

Measurements of pH and Ca^{2+}, Na$^+$, K$^+$ and SO$_4^{2-}$ concentrations were also carried out on binder suspensions prepared by mixing crushed cement paste samples (cured for 6 months and 1 year in sealed bag at 20 °C) with ultrapure water (liquid to solid ratio of 9 mL/g) and stirring for 24 h. Experiments and measurements were carried out under nitrogen atmosphere to prevent carbonation.

4 × 4 × 16 cm specimens of cement pastes (blends B, T1 and T2) with a W/C = 0.4 were prepared and cured for 7 months at 95% relative humidity and constant temperature (20 °C). They were then cut in 3 cm-thick slices and put into 1.8 L cylindrical tanks filled with deionized water for calcium leaching tests [16]. All trials were carried out at constant temperature (20 °C) and pH (7). This latter was regulated automatically by adding nitric acid at a concentration of 0.25 mol/L to the leaching solution. To avoid carbonation of the samples during the tests, nitrogen gas was continuously injected in the tanks. The samples were protected from lateral degradation by a polymer coating, and the external attack occurred on two parallel and opposite faces only in one direction. To maintain experimental conditions constant during the tests, the solution was renewed at regular intervals, in connection with the quantity of added nitric acid. This quantity was directly related to the amount of calcium leached from the paste. The Ca^{2+} and SO$_4^{2-}$ concentrations, in the leaching solution, were determined by ionic chromatography, the silicate concentration was measured by ICP-AES, and the OH$^-$ concentration was inferred from the pH values. The solutions were constantly stirred to avoid any local increase in concentration. The mineralogy of the leached zone was assessed by scraping progressively the samples from the external surface to the center of the slices using a micromilling machine [17]. The abraded thickness was not monitored very accurately but the residual thickness after scraping was measured to within micrometer. With the help of XRD (Pan

Table 5
Evolution of the portlandite content (weight %) of the different cement pastes

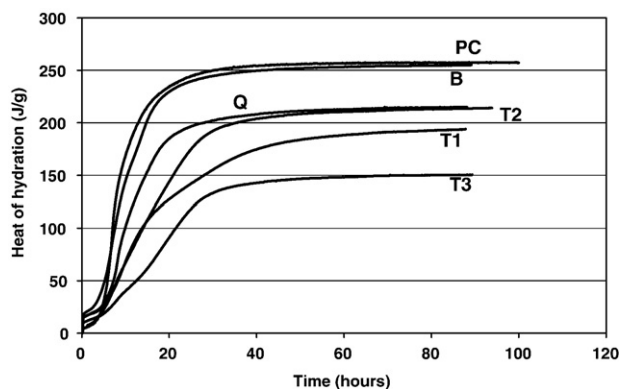|	PC	CEM V	B	T1	T2	T3	Q
1 month	21.6	10.4	4.8	2.0	3.7	0	3.3
2 months	24.7	9.6	5.2	0.3	3.5	0	1.6
3 months	21.7	8.8	2.9	0	2.5	0	0
6 months	20.1	7.9	3.6	0	2.0	0	0
1 year	18.8	6.1	2.0	0	1.0	0	0

Fig. 1. Heat of hydration of low-pH blended cements and Portland cement (PC).

Analytical Xpert Pro-Copper anode $\lambda_{K\alpha1} = 1.54056$ Å) analyses, it was possible by this way to determine the crystallized phases within slices of approximately 100 µm thick, parallel to the leached surface.

3. Results and discussion

3.1. Hydration of cement pastes

3.1.1. Characterization of the solid

3.1.1.1. Portlandite content.
Evolution with time of the portlandite content, measured by TG-DTA, in the pastes is shown in Table 5.

Portlandite was totally depleted in blends T1 and Q after 3 months of curing, while it could still be detected after 1 year in blend T2. T1 and T2 differed only by the fact that FA (in T1) was replaced by slag in T2. Thus, FA revealed more effective to consume portlandite, which may be explained by its higher silica content. Quite unexpected results were obtained for blend B: despite its high SF content (40%), the most reactive product of the investigated pozzolans, portlandite was still present after 12 months. This resulted from an inhomogeneous dispersion of SF in the paste, as it will be shown later from the SEM observations. According to Hong and Glasser [12], SF up to 15–20% cement replacement should be enough to react with all portlandite if properly dispersed. Portlandite was not detected at any age in sample T3, which may result from its very low content of clinker (20%). In the commercial CEM V cement

paste, the amount of portlandite decreased, but more slowly than in the low-pH cement pastes which all contained silica fume. Thus, properly dispersed SF was the most effective pozzolan for a rapid depletion of portlandite. These results were supported by XRD analyses.

3.1.1.2. Heat of hydration.
The total heat of hydration of most low-pH cements (excepting B) was lower than that of PC (T2: 215 J/g, T1: 195 J/g, T3: 150 J/g, PC: 250 J/g) (Fig. 1).The hydration rate was lower in the acceleratory period, and it decreased when the substitution level for clinker increased. This result is consistent with data from the literature. (*i*) The heat production is enhanced by a small addition (10%) of SF [18], but decreased by a large addition due to PC dilution. (*ii*) Calorimetric studies show that FA retards the reaction of alite in the early stage of hydration [19–22]. (*iii*) In slag cements, slag reacts considerably more slowly than alite, thus reducing the heat output [23]. For similar cement replacement levels, the heat release of blend Q was smaller than that of blend B, which was due to the fact that CEM V hydration was less exothermic than PC hydration. In the same way, the heat output of fly ash-containing blend T1 was smaller than that of slag-containing blend T2.

3.1.1.3. Porosity.
Mercury Intrusion Porosity was used to characterize cement pastes after 1 and 3 months of curing. Whatever the age of the sample, adding fly ash and slag resulted in an increase in the total porosity (highest values occurred in blends T1 and T3, Table 6). While the porosity of the commercial cement pastes (PC and CEM V) decreased with time, that of the low-pH cement pastes remained almost constant over the 3-month period of the study. However their pore size distribution showed a progressive refinement. The fraction of pores with a diameter below 20 nm (gel pores, associated with C–S–H) increased with time and was much more important than that measured for PC.

Table 7
Mineralogy of the low-pH cement pastes shown by XRD (sealed bag, 20 °C)

Components of the pastes (age: 6 months)
B   C–S–H–Ca(OH)$_2$–ettringite–C$_2$S–C$_3$S–hematite–calcite–quartz
T1   C–S–H–ettringite–C$_2$S–C$_3$S–hematite–calcite–quartz–mullite–magnetite
T2   C–S–H–Ca(OH)$_2$–ettringite–C$_2$S–C$_3$S–calcite–hydrotalcite
T3   C–S–H–ettringite–C$_2$S–C$_3$S–calcite–hydrotalcite
Q   C–S–H–ettringite–C$_2$S–C$_3$S–calcite–quartz–hydrotalcite

Table 6
Total porosity of cement pastes (volume %) and pore size distribution (diameter) of 1-month-old and 3-month-old cement pastes (% of total porosity)

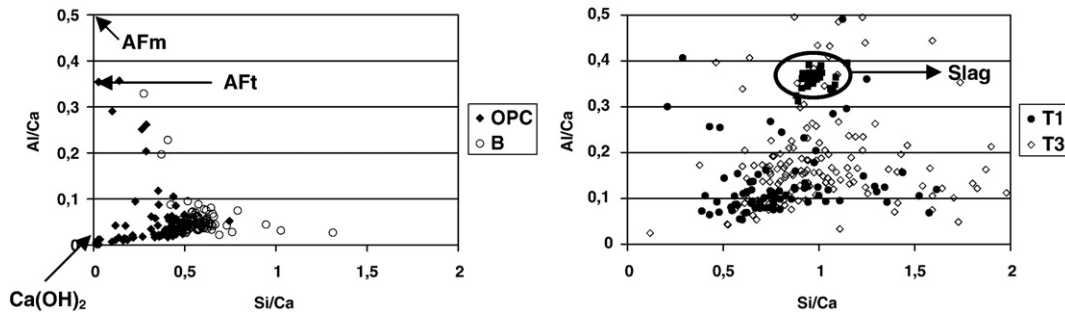|		PC	CEMV	B	T1	T2	T3	Q
1 month	Total porosity	30.9	33.9	30.2	37.1	34.9	37.3	33.9
	>100 nm	26.0	14.4	14.6	10.1	13.7	10.2	23.6
	20–100 nm	54.2	27.4	35.4	42.4	22.7	39.1	49.8
	<20 nm	19.8	58.2	50.0	47.5	63.6	50.7	26.5
3 months	Total porosity	25.3	28.9	31.9	36.0	32.6	37.5	36.0
	>100 nm	4.7	5.3	16.0	8.2	12.3	9.0	17.8
	20–100 nm	63.0	9.7	29.9	32.6	117.5	31.9	33.7
	<20 nm	32.4	85.0	54.1	59.2	70.2	59.1	48.5

Fig. 2. Al/Ca vs Si/Ca atom ratios for individual X-ray microanalyses of Portland cement paste and low-pH cement pastes (age: 6 months).

3.1.1.4. Mineralogy of PC and low-pH binder pastes. The mineralogy of the pastes was investigated by XRD after 6 months of curing in sealed bag (Table 7). All samples contained anhydrous phases (alite, belite), ettringite and traces of calcite. Portlandite was detected in blends B and T2, and hydrotalcite in slag-containing blends (T2, T3, Q). Four of them (PC, B, T1 and T3) were analysed using EDS [24]. Fig. 2 shows a plot of Al/Ca against Si/Ca ratios for individual X-ray microanalyses from several parts of the microstructures of the samples. Most analyses on the PC paste clustered for Si/Ca ratio between 0.4 and 0.5 and corresponded to C–S–H. The spots analysed were not chosen at random, thus the number of portlandite (CH, Si/Ca=0) was underestimated. The analyses intermediate between those of C–S–H and CH, AFt or AFm probably corresponded to mixtures below the micrometer scale of C–S–H and the relevant phase. Paste B was characterized by C–S–H with a higher Si/Ca ratio (within the range 0.5–0.6). Mixtures with portlandite were scarce in the blended cement pastes. Analyses performed on cement pastes T3 and T1 showed much more variation. For most spots in the C–S–H zone, both the Si/Ca and Al/Ca ratios were increased, which could be related to the higher silica and alumina contents of these systems as compared to PC (Table 4). These results could be compared with other researchers' work. Richardson et al. [25,26] have shown that in a slag/PC blend, the S/C ratio of the C–S–H increases with the proportion of slag from around 0.55 for plain PC cement paste to 0.8–0.9 in the extreme case of a paste of an alkali-activated slag containing no Portland cement. For a blend comprising 50% slag, values around 0.65 have been obtained. As for a 3-day-old cement paste containing fly ash, it has been reported that S/C and A/C are higher than in pure Portland cement pastes [9,10,27–30].

3.1.2. Characterization of the interstitial solution

The pore solution pH values of the blended pastes decreased with time and were within the range [11.7–12.4] after 1 year of hydration (Table 8). They still exceeded the target pH of 11, but were reduced by more than one unit as compared to PC and CEM V cement pastes. Differences could be noticed between the blends: the smallest pH values were recorded for T1 and T3, and the highest for blends B and T2. Comparing data relative to blends T1 and T2 showed that the association of SF and FA

(blend T1) led to a stronger pH reduction than the association of SF and slag (blend T2). Given the difficulty to extract pore solution under pressure, two protocols were compared: (*i*) pore solution extraction, and (*ii*) preparation of a suspension by mixing ground cement paste with ultrapure water for 24 h (method already investigated by Räsänen and Pentala [31]). The pH values measured in both cases were very similar except for PC and CEM V. This result will be discussed later in this section.

The compositions of the pore solution extracted from 2, 6 and 12-month-old samples are presented in Table 9. The extracted interstitial solutions of the low-pH blends exhibited strongly reduced (up to a factor 20 to 200) contents of Na^+ and K^+ as compared with PC. The calcium concentrations were in fairly good agreement with C–S–H equilibrium data (Fig. 3) for all low-pH blends, excepting cement paste Q, which had a higher content of alkalis. In the low-pH blends, the pore solution chemistry was thus controlled by the C–S–H dissolution. The good agreement between the two protocols of pH measurement could then be explained as follows. The dilution factor in the suspension (W/C=9 instead of 0.5 in cement pastes) was low enough to prevent total dissolution of C–S–H and the equilibrium concentrations thus remained the same. On the other hand, the pore solution pH of PC and CEM V was dominated by highly soluble alkali hydroxides and pH was above 13. Preparing a suspension caused a dilution of the alkalis, and thus a pH reduction. For T2 and B, quite unexpected results were obtained after 1 year of curing. Despite the presence of portlandite as shown by XRD and

Table 8
Pore solution pH of the cement pastes

pH	EIS 2 months	EIS 6 months	CS 6 months	EIS 1 year	CS 1 year
PC		13.2	12.6	13.1	12.6
CEM V		13.4	12.6	13.3	12.4
B	12.4	12.6	12.5	12.2	12.4
T1	12.4	12.2	12.2	11.7	11.7
T2	12.3	12.4	12.4	12.2	12.2
T3	12.1	12.0	12.0	11.7	11.8
Q	12.5	12.5	12.4	12.1	12.0

Measurements carried out on extracted interstitial solutions (EIS) and cement suspensions (CS).

Table 9
$[Na^+]$, $[K^+]$, $[Ca^{2+}]$ and $[SO_4^{2-}]$ (mmol/L) in the extracted interstitial solutions

	2 months				6 months				12 months			
	Na^+	K^+	Ca^{2+}	SO_4^{2-}	Na^+	K^+	Ca^{2+}	SO_4^{2-}	Na^+	K^+	Ca^{2+}	SO_4^{2-}
PC					77.9	71.8	0.2	0.8	92.9	77.1	0.02	1.1
CEMV					47.1	172.0	0.5	2.4	72.5	241.5	0.03	3.9
B	4.7	3.3	8.9	0.4	3.1	3.2	9.5	0.2	3.1	2.7	5.4	0.3
T1	2.0	1.1	11.0	ND	3.8	1.4	3.8	0.2	4.5	1.9	1.6	1.4
T2	3.6	1.4	7.3	ND	3.0	1.7	8.4	0.1	3.0	1.0	5.8	0.2
T3	3.5	1.3	4.5	0.2	2.9	1.5	4.7	0.6	2.9	1.1	4.2	0.9
Q	8.7	15.9	1.5	ND	7.5	11.5	3.9	0.1	7.3	9.3	0.1	0.3

ND: below the detection limit.

TGA, the pH of the extracted solutions was below the portlandite equilibrium pH. This might be explained by an inhomogeneity of the material, which would locally contain portlandite, this latter being isolated from the interstitial solution by the growing hydrates.

The reduced alkali content in the pore solution of low-pH cements pastes could result from various factors: the enhanced sorption capacity of the C–S–H gel due to its increased Si/Ca ratio, the occurrence of badly dispersed silica fume aggregates, since amorphous silica is known to have adsorption properties which result from the hydroxylation of its surface [12,34–36] and, for blends T2 and T3, the possible formation of magnesium silicate hydrate gel (magnesium coming from the slag) which has been identified as an effective sorbent for potassium [37,38]. The sorption potential of other phases such as hydrotalcite and strätlingite has still to be elucidated.

Additional, experiments were performed on the cement suspensions (liquid to solid ratio equal to 9 mL/g): once equilibrium was reached, half of the liquid phase was replaced by ultrapure water, and the Na^+ and K^+ concentrations were followed as a function of time. They increased to restore equilibrium and finally reached their initial values, which indicated that under these conditions, the sorption of Na^+ and K^+ by the solid phase was reversible.
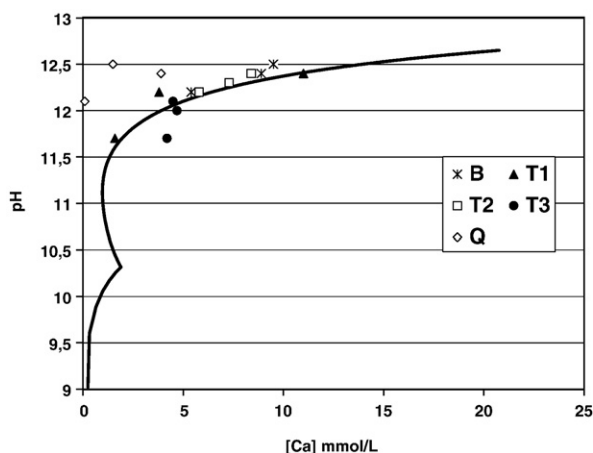
Fig. 3. Equilibrium model of pure C–S–H at 20 °C according to Nonat [32,33] with data relative to 2, 6 and 12-month-old low-pH cement pastes.

3.2. Leaching of cement pastes

3.2.1. Characterization of the degraded solid

From samples leached for a 4-month period, we tried to estimate the position of the degradation front. Portlandite is a good indicator for the location of the degradation front for common PC-based materials [39–41]. However, in this study, a difficulty arose from the fact that there was no or little portlandite in many of the pastes studied. Different techniques were thus combined: optical microscopy observations, SEM observations and X-ray microanalysis, as well as X-ray diffraction of the leached surface.

First, phenolphtaleine tests were carried out. The degraded thickness was visually estimated by optical microscopy observations as shown in Fig. 4. On these images, two zones could be distinguished. The bright zone was a part of the cement paste which did not colour phenolphtaleine in purple, which meant that the pH in this zone was below 10. Whatever the sample, the measured thickness of pH < 10 was between 600 and 700 μm after 4 months of leaching.

The second approach was to use chemical contrasts from SEM/BSE images, the density of the degraded zone being lower than that of the sound core due to decalcification. A sharp transition was effectively observed between a bright zone (sound core) and a dark one (degraded material) for blends B, T1 and T2. The degradation depth was within the range 900–1200 μm. For blend T3 however, locating the degradation front was much more difficult, which may have resulted from its very low content of clinker (20%). Ca- and Si-mapping clearly showed the decalcification of the cement pastes near the surface exposed to leaching while the silica content seemed to remain quite constant whatever the considered depth. These investigations were supplemented by performing EDS microanalyses to estimate the Ca/Si molar ratio of the pastes as a function of the distance from the leached surface (Fig. 5). Three zones could be defined. The first one, near the surface, was characterized by a very low and almost constant Ca/Si ratio (0.3 to 0.4 for all blends). Its depth varied from 200 to 600 μm depending on the samples (Table 10). The second one corresponded to a transition: the Ca/Si ratio gradually increased. It was much larger for blend T1 (> 1000 μm) than for the other samples (400 to 600 μm). The third one, in which the Ca/Si ratio showed again little variation, could be attributed to the sound core. The
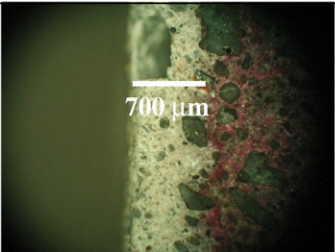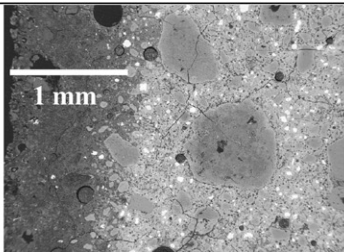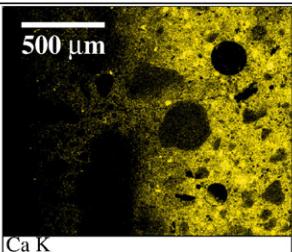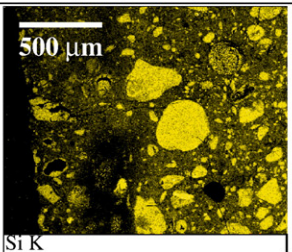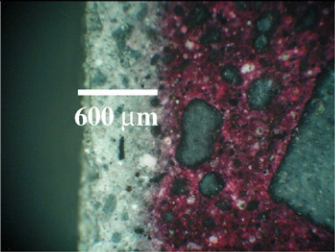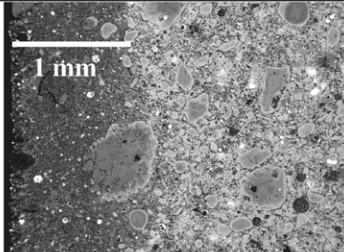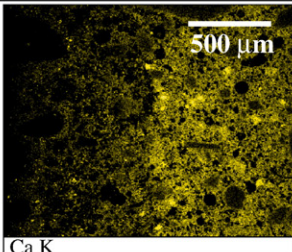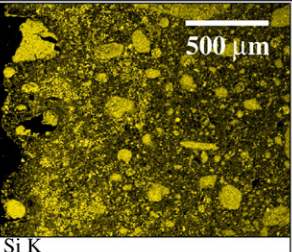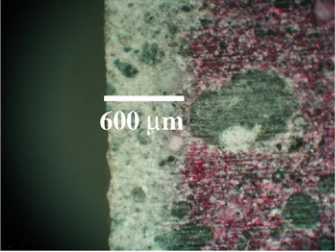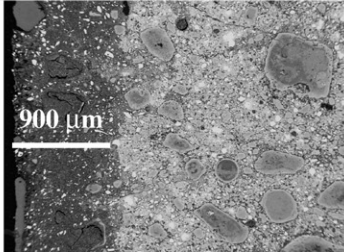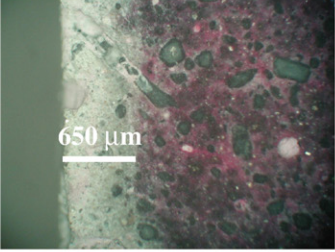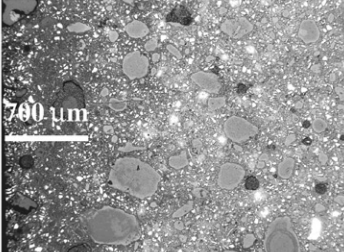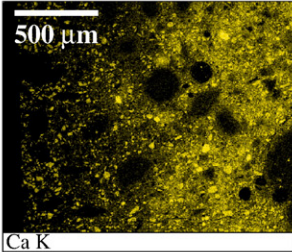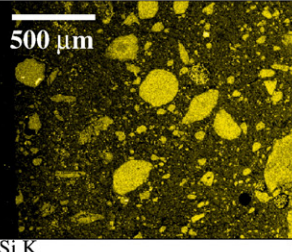
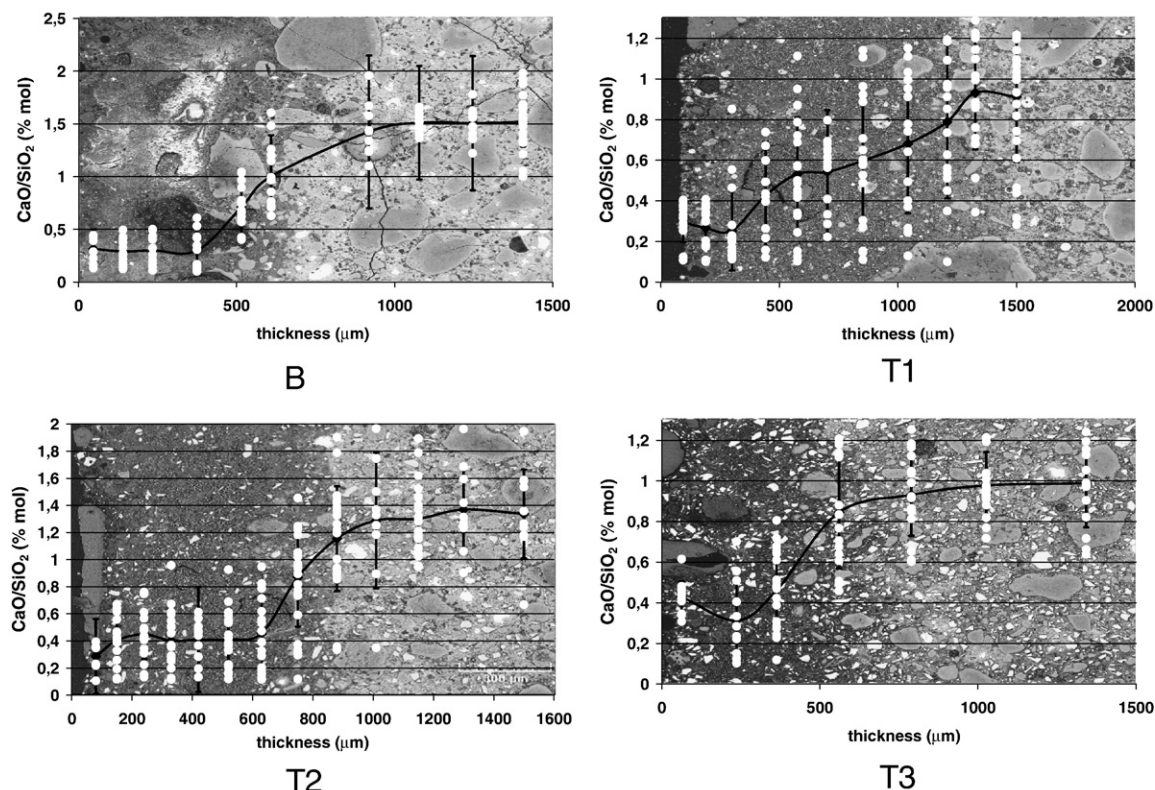| Blend	Optical microscopy observations	SEM observations (BSE)	SEM with X-ray microanalysis (Map of Ca)	SEM with X-ray microanalysis (Map of Si)
B				
T1				
T2				
T3				

Fig. 4. Pictures of the samples (B, T1, T2 and T3) after 4 months of leaching.

Fig. 5. C/S ratio evolution vs degraded thickness of the cement pastes (B, T1, T2 and T3). Each point represents an EDS analysis. The curves are plotted from the average values obtained for each investigated depth (erratic points being excluded) and errors bars are calculated from the standard deviation.

Ca/Si average value depended on the sample: 1.5 for blend B, 0.9 for blend T1, 1.4 for blend T2 and 1.0 for blend T3. The total degradation depth (zones 1 and 2) thus ranged between 800 μm (blend T3) to 1300 μm (blend T1), which was in rather good agreement with the estimations derived from BSE pictures, but not with those inferred from optical microscopy. In that latter case, the change in colour of phenolphtaleine occurred at pH ≈ 10, which was lower than the equilibrium pH of the C–S–H from the sound core. The change in colour of phenolphtaleine thus occurred in the degraded zone, but near the sound core.

In a third approach, XRD analyses were carried out on the samples surface which was scraped off step by step (thickness ≈ 100 μm for each step) to obtain XRD profiles (Fig. 6). Several mineralogical evolutions were noticed near the leached surface:

- decrease in the magnitude of the C–S–H peak, which corresponded to a progressive decalcification of the material,
- disappearance of portlandite for pastes B and T2,
- disappearance of ettringite whatever the sample,
- enrichment in an hydrotalcite-like phase for pastes T2 and T3 (containing slag),
- partial (paste B) or total (pastes T1, T2 and T3) depletion of C_3S and C_2S, due to dissolution and possibly hydration.

Table 10 summarises the results inferred from the different characterization techniques. We tried to estimate the degradation depth from the disappearance of portlandite and/or ettringite.

Although the accuracy was not very good, the results were rather consistent with the SEM observations.

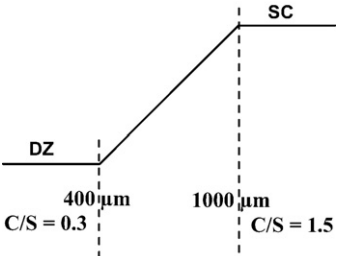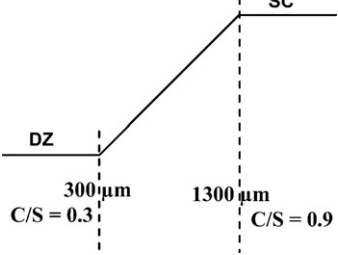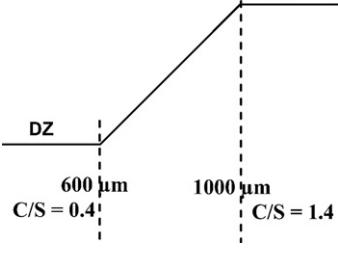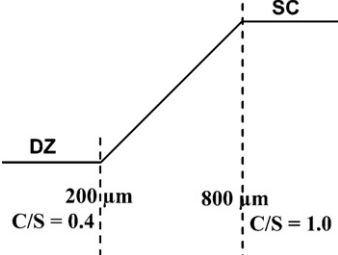### 3.2.2. Characterization of the leaching solution

Figs. 7 and 8 show the cumulative quantities of OH^- and Ca^{2+} released in the leaching solution as a function of the square root of time for samples B, T1, T2 and T3 while Table 11 summarises the fluxes of the released species derived from the slopes of the previous curves.

Blend B showed the highest decalcification rate, and blends T1 and T3 the smallest. The rate values could be compared with reference data: decalcification of the low-pH blends was much slower than that of PC (13 ± 2 mmol/dm^2/day$^{0.5}$) and rather similar to that of CEM V (3 ± 0.4 mmol/dm^2/day$^{0.5}$) [42]. The ratios between the hydroxyl and calcium fluxes were different from 2 (1.86 for blend B, 1.85 for blend T1, 2.11 for blend T2 and 1.96 for blend T3). Additional analyses performed for sample B showed that the Ca^{2+} flux was not only balanced by the release of OH^- but also by that of silica and sulphate anions (resulting from the destabilisation of ettringite). Results showed that for a 21 days leaching test, the OH^-/Ca^{2+} flux ratio was equal to 1.90 and the $(OH^- + HSiO_3^- + 2 SO_4^{2-})/(Ca^{2+})$ flux ratio was equal to 2.11 (SO_4^{2-} flux = 0.13 ± 0.01 mmol/dm^2/day$^{0.5}$ and $HSiO_3^-$ flux = 0.76 ± 0.02 mmol/dm^2/day$^{0.5}$). These values could be compared to those from Adenot for a PC paste submitted to leaching under the same conditions (SO_4^{2-} flux of 0.22 mmol/dm^2/day$^{0.5}$, $HSiO_3^-$ flux of 0.29 mmol/dm^2/day$^{0.5}$) [16]. The SO_4^{2-} fluxes were quite similar, while the $HSiO_3^-$ flux

Table 10
Summary of results obtained by optical microscopy and SEM/BSE — zone of appearance of portlandite and ettringite in the leaching cement pastes

Blends	Optical microscopy observations	SEM/BSE observation	Schematic graph resulting from C/S ratio evolution	Zone of appearance of portlandite	Zone of appearance of ettringite
B	700 μm	1000 μm	SC; DZ; 400 μm C/S = 0.3; 1000 μm C/S = 1.5	[1100–1300]	[850–1050]
T1	600 μm	1000 μm	SC; DZ; 300 μm C/S = 0.3; 1300 μm C/S = 0.9	–	[800–1000]
T2	600 μm	900 μm	SC; DZ; 600 μm C/S = 0.4; 1000 μm C/S = 1.4	[700–100]	[700–1000]
T3	650 μm	too indistinct	SC; DZ; 200 μm C/S = 0.4; 800 μm C/S = 1.0	–	?

DZ = degraded zone, SC = sound core.

of paste B was more important due to the much higher silica content of the binder.

4. Conclusions

Cement pastes prepared with five blends containing high amounts of silica fume, fly ash and/or slag were investigated. Their main properties can be summarised as follows:

- reduced heat of hydration as compared to PC,
- refined porosity, although the total porosity remained higher than that of the reference,
- pore solution with a pH comprised between 11.7 and 12.4 after 1 year of curing, and with very strongly reduced (up to a factor 20 to 200) Na^+ and K^+ concentrations as compared to a PC reference,
- decalcification rate under leaching by pure water reduced by a factor 4 as compared to PC,
- degraded thickness after 4 months of leaching ranging from 800 μm (ternary blend with a high slag content) to 1300 μm (ternary blend with fly ash).

Different methods were compared to estimate the position of the degradation front. Estimating the Ca/Si ratio evolution from the sound core to the surface submitted to leaching using SEM–EDS analysis as well using the chemical contrast from SEM/BSE pictures seemed to be the most reliable techniques.
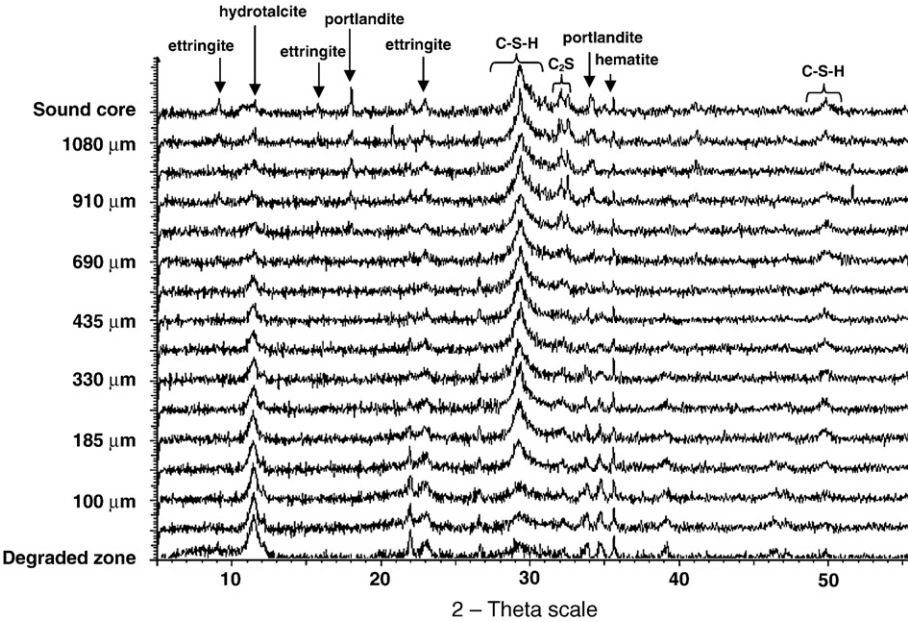
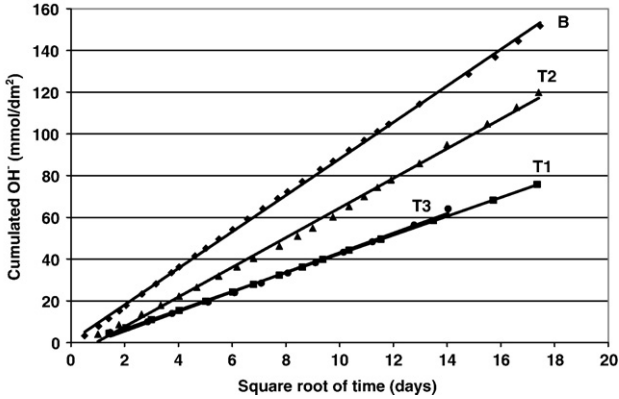Fig. 6. XRD pattern of the degraded zone of paste T2 (from the surface (bottom) to the sound core (top)).

Fig. 7. OH⁻ released during leaching of cement pastes in pure deionized water (pH 7, 20 °C).
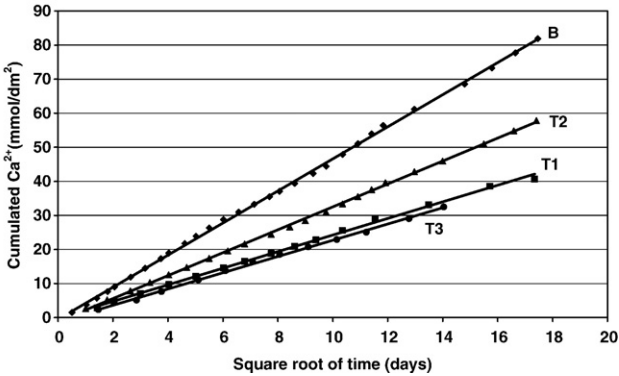

Fig. 8. Ca²⁺ released during leaching of cement pastes in pure deionized water (pH 7, 20 °C).

Table 11
Ca^{2+} and OH^- fluxes measured during the leaching experiments (inferred from the graphs of Figs. 7 and 8)

$mmol/dm^2/day^{0.5}$	OH^- flux	Ca^{2+} flux
B	8.744 ± 0.044	4.709 ± 0.023
T1	4.508 ± 0.014	2.437 ± 0.030
T2	7.107 ± 0.083	3.363 ± 0.017
T3	4.695 ± 0.080	2.386 ± 0.031

Positive fluxes refer to outward fluxes.

The pore solution chemistry of the low-pH cement pastes was dominated by the C–S–H dissolution. An alternative method to pore solution expression for low-pH blends was thus proposed to estimate the pH of the interstitial solution. pH could be more simply measured on a cement suspension (liquid to solid ratio of 9 mL/g) stirred for 24 h under nitrogen atmosphere.

Future work will be focused on modelling leaching experiments by taking into account both chemical reactivity and transport through diffusion and the sorption of alkali by the cement pastes will be studied more accurately.

Acknowledgements

References

[1] ANDRA, 2005 Report on Clay — Evaluating the Feasibility of a Geological Repository in Clay Formation, ISBN: 2-951-0108-8-5, 2005, p. 238.

[2] P. Sellin, F. Karlsson, L. Werme, K. Spahiu, I. Puigdomenech, Effect of pH on the safety of KBS-3 deep repository and the confidence in the safety assessments, Proc. Workshop on Qualification of Low-pH Cement for a Geological Repository, Stockholm, Sweden, October 15–16, 2003.

[3] C. Cau-dit-Coumes, S. Courtois, D. Nectoux, S. Leclercq, X. Bourbon, Formulating a low-alkalinity, high-resistance and low-heat concrete for radioactive waste repositories, Cem. Concr. Res. 36 (2006) 2152–2163.

[4] M.N. Gray, B.S. Shenton, For better concrete, take out some of the cement, Proc. 6th ACI/CANMET Symposium on the Durability of Concrete, Bangkok, Thailand, 1998, May 31 to June 5, 1998.

[5] B. Lagerblad, High performing concrete with low pH as bore hole plugging material, Produced for SKB Seminar on borehole plugging, Äspö, February 27th 2003, 2003.

[6] K. Iriya, A. Matsui, M. Mihara, Study on applicability of HFSC for radioactive waste repositories, Radioactive Waste Management and Environmental Remediation, ASME Conference, Nagoya, Japan, September 16–30 1999, 1999.

[7] U. Vuorinen, J. Lehikoinen, Low-pH grouting cements — results of leaching experiments and modelling, 2nd low-pH Workshop, Madrid, Spain, June 15–16, 2005.

[8] S. Urhan, Alkali silica and pozzolanic reactions in concrete. Part 1: interpretation of published results and an hypothesis concerning the mechanism, Cem. Concr. Res. 17 (1987) 141–152.

[9] S.A. Rodger, G.W. Groves, The microstructure of tricalcium/silicate pulverized-fuel ash blended cement pastes, Adv. Cem. Res. 1 (1988) 84.

[10] P.L. Rayment, The effect of pulverised fuel ash on the C/S molar ratio of alkali content of calcium silicate hydrates in cement, Cem. Concr. Res. 12–2 (1982) 133–140.

[11] J. Duchesne, M.A. Bérubé, The effectiveness of supplementary cementing materials in suppressing expansion due to ASR — another look at the reaction mechanism — Part 2 — pore solution chemistry, Cem. Concr. Res. 24–2 (1994) 221–230.

[12] S.-Y. Hong, F.P. Glasser, Alkali sorption by C–S–H gels. Part II. Role of alumina, Cem. Concr. Res. 32 (2002) 1101–1111.

[13] H.J.H. Brouwers, R.J. Van Eijk, Alkali concentrations of pore solution in hydrating OPC, Cem. Concr. Res. 33 (2003) 191–196.

[14] S.-Y. Hong, F.P. Glasser, Alkali binding in cement pastes. Part I. The C–S–H phase, Cem. Concr. Res. 29 (1999) 1893–1903.

[15] S.A. Stronach, F.P. Glasser, Modelling the impact of abundant geochemical components on the phase stability and solubility of the $CaO–SiO_2–H_2O$ system at 25 °C: Na^+, K^+, SO_4^{2-}, Cl^- and CO_3^{2-}, Adv. Cem. Res. 36 (1997) 167–181.

[16] F. Adenot, Durabilité des bétons: caractérisation et modélisation des processus physiques et chimiques de dégradation du ciment Ph D Thesis, Université d'Orléans, France, 1992.

[17] D. Planel, Les effets couples de la précipitation d'espèces secondaires sur le comportement mécanique et la dégradation chimique des bétons, Ph D Thesis, Université de Marne La Vallée, France, 2002.

[18] E.H. Kadri, R. Duval, Effect of ultrafine particles on heat of hydration of cement mortars, ACI Mater. J. (2002) 138–142.

[19] A. Ghose, P.L. Pratt, in: S. Diamond (Ed.), Effects of Flyash Incorporation in Cement and Concrete, Materials Research Society, University Park, 1981, p. 82.

[20] Y. Halse, P.L. Pratt, J.A. Dalziel, W.A. Gutteridge, Development of microstructure and other properties in flyash OPC systems, Cem. Concr. Res. 14 (1984) 491.

[21] I. Jawed, J. Skalny, in: S. Diamond (Ed.), Effects of flyash incorporation in cement and concrete, Materials Research Society, University Park, 1981, p. 60.

[22] F. Wei, M.W. Grutzeck, D.M. Roy, The retarding effects of fly ash upon the hydration of cement pastes: the first 24 hours, Cem. Concr. Res. 15 (1985) 174–184.

[23] H.F.W. Taylor, Cement Chemistry, in: T. Telforf (Ed.), London, 1997, p. 263.

[24] C. Famy, A.R. Brough, H.F.W. Taylor, The C–S–H gels of Portland cement mortars: Part I. The interpretation of energy-dispersive X-ray microanalysis from scanning electron microscopy, with some observations on C–S–H, AFm and Aft phase compositions, Cem. Concr. Res. 33 (2003) 1389–1398.

[25] I.G. Richardson, G.W. Groves, Microstructure and microanalysis of hardened cement pastes involving ground granulated blast-furnace slag, J. Mater. Sci. 27 (1992) 6204.

[26] I.G. Richardson, Tobermorite/jennite- and tobermorite/calcium hydroxide-based models for the structure of C–S–H: applicability to hardened pastes of tricalcium silicate, β-dicalcium silicate, Portland cement, and blends of Portland cement with blast-furnace slag, metakaolin, or silica fume, Cem. Concr. Res. 34 (2004) 1733–1777.

[27] M. Regourd, B. Mortureux, H. Hornain, Fly ash, silica fume, slag and other mineral by-products in concrete, in: V.M. Malhotra (Ed.), Sp. Publ. SP79, vol. 2, American Concrete Institute, Detroit, MI, 1983, p. 847.

[28] H.F.W. Taylor, K. Mohan, G.K. Moir, Analytical study of pure and extended Portland cement pastes: II, fly ash- and slag-cement pastes, J. Am. Ceram. Soc. 68 (1985) 685–690.

[29] H. Uchikawa, Effect of blending components on hydration and structure formation, 8th ICCC, vol. 1, 1986, p. 249.

[30] A.M. Harrisson, N.B. Winter, H.F.W. Taylor, An examination of some pure and composite Portland cement pastes using scanning electron microscopy with X-ray analytical capability, 8th ICCC, vol. 3, 1986, pp. 170–175.

[31] V. Räsänen, V. Penttala, The pH measurement of concrete and smoothing mortar using a concrete powder suspension, Cem. Concr. Res. 34 (2004) 813–820.

[32] A. Nonat, The structure and stoichiometry of C–S–H, Cem. Concr. Res. 34 (2004) 1521–1528.

[33] R. Barbarulo, Comportement des matériaux cimentaires: Action des sulfates et de la température, Ph D Thesis, Ecole Normale Supérieure Cachan et Faculté des études supérieures de l'Université Laval, Québec, (2002).

[34] M.C.G. Juenger, C.P. Ostertag, Alkali-silica reactivity of large silica fume-derived particles, Cem. Concr. Res. 34 (2004) 1389–1402.

[35] J.A. Larbi, A.L.A. Fraay, J.M.J.M. Bijen, The chemistry of the pore fluid of silica fume-blended cement systems, Cem. Concr. Res. 20 (1990) 506–516.

[36] D. Bonen, S. Diamond, Occurrence of large silica fume-derived particles in hydrated cement paste, Cem. Concr. Res. 22 (1992) 1059–1066.

[37] D.R.M. Brew, F.P. Glasser, Synthesis and characterisation of magnesium silicate hydrate gels, Cem. Concr. Res. 35 (2005) 85–98.

[38] D.R.M. Brew, F.P. Glasser, The magnesia–silica gel phase in slag cements: alkali (K, Cs) sorption potential of synthetic gels, Cem. Concr. Res. 35 (2005) 77–83.

[39] M. Buil, E. Revertegat, J. Oliver, A model of the attack of pure water or undersaturated lime solutions on cement, in: T.M. Gilliam, C.C. Wiles (Eds.), American Society for Testing and Materials, West Conshohocken, USA, 1992, pp. 227–241.

[40] F. Adenot, M. Buil, Modelling of the corrosion of the cement paste by deionized water, Cem. Concr. Res. 22 (1992) 489–495.

[41] F. Adenot, J. Maury, C. Richet, Long-term prediction of concrete durability in radioactive waste management: influence of the pH of the aggressive solution, in: A. Al-Manaseer, S. Nagataki, R.C. Joshi (Eds.), Int. Conf. On Eng. Mat., Ottawa, Canada, vol. 2, 1997, pp. 117–128.

[42] C. Richet, C. Gallé, P. Le Bescop, H. Peycelon, S. Bejaoui, I. Tovena, I. Pointeau, V. L'Hostis, P. Lovera, Synthèse des connaissances sur le comportement à long terme des bétons — Applications aux colis cimentés, CEA-R-6050, Saclay, France, 2004.

[43] A. Krönlof, Injection grout for deep repositories, low pH cementitious grout for larger fractures, testing technical performance of materials, Proc. Workshop on Qualification of Low pH Cement for a Geological Repository, Stockholm, Sweden, October 15–16, 2003.